Structural and optical properties of InAs/AlAsSb quantum dots with GaAs(Sb) cladding layers

Paul J. Simmonds,[1,a)] Ramesh Babu Laghumavarapu,[2] Meng Sun,[2] Andrew Lin,[2] Charles J. Reyner,[2] Baolai Liang,[1] and Diana L. Huffaker[1,2]
[1]*California NanoSystems Institute, UCLA, Los Angeles, California 90095, USA*
[2]*Department of Electrical Engineering, UCLA, Los Angeles, California 90095, USA*

(Received 23 April 2012; accepted 30 May 2012; published online 14 June 2012)

We investigate the effect of $GaAs_{1-x}Sb_x$ cladding layer composition on the growth and properties of InAs self-assembled quantum dots surrounded by $AlAs_{0.56}Sb_{0.44}$ barriers. Lowering Sb-content in the $GaAs_{1-x}Sb_x$ improves the morphology of the InAs quantum dots and reduces cladding layer alloy fluctuations. The result is a dramatic increase in photoluminescence intensity from the InAs quantum dots, with a peak at 0.87 eV. The emission energy exhibits a cube root dependence on excitation power, consistent with the type-II band alignment of the quantum dots. The characteristics of this quantum dot system show promise for applications such as intermediate band solar cells. © *2012 American Institute of Physics*. [http://dx.doi.org/10.1063/1.4729419]

The intermediate band solar cell (IBSC) is a promising candidate for next-generation, high-efficiency photovoltaics.[1,2] In an IBSC, a miniband is created within the semiconductor band gap enabling the simultaneous absorption of photons with multiple energies. An IBSC peak efficiency of 63.2% is predicted, a significant increase from the 40.7% limit calculated for traditional single-gap solar cells.[2] Self-assembled quantum dots (SAQDs) provide an attractive way to create an intermediate band (IB),[3,4] and much IBSC research has focused on InAs/GaAs and GaSb/GaAs SAQDs.[5,6] However, although InAs/GaAs is perhaps the most widely studied SAQD system, other materials may be better suited to the realization of high-efficiency IBSCs.[7–9]

InAs(Sb) SAQDs surrounded by $AlAs_{0.56}Sb_{0.44}$ barriers (lattice matched to InP, hereafter referred to as AlAsSb) were identified by Levy *et al.* as having several characteristics well suited to IBSC applications.[10] Band gaps of ~0.7 and ~1.22 eV are available for QD and barrier, respectively. These band gaps are close to the optimal values calculated for IBSCs using the blackbody spectrum,[10,11] although detailed analysis by Bremner *et al.* using the terrestrial solar spectrum shows that lower (higher) QD (barrier) band gaps may be more efficient.[12] Furthermore, InAs(Sb)/AlAsSb SAQDs have type-II band alignment offering strong electron confinement, while the valence band (VB) offset at the InAs(Sb)/AlAsSb interface is small (tending to zero for certain QD compositions).[10] For well-confined electron systems, zero VB offsets or weakly type-II band alignments are preferred for IBSCs since they eliminate the possibility of IB formation for electrons and holes in the same structure. Coexistence of electron and hole IBs would increase the radiative recombination probability, hence reducing IBSC efficiency.[10] Small type-II VB offsets also mean weak hole localization outside the SAQD,[13] with potential benefits for IBSCs including lower carrier recombination rates, increased carrier lifetimes, and more efficient carrier extraction. Stacking multiple layers of QDs would compensate for any reduction in photon absorption associated with the type-II band alignment. Lower strain for certain compositions in the InAs(Sb)/AlAsSb system means that unlike archetypal InAs/GaAs SAQDs, stacking QD layers may be possible without the complication of adding strain-compensation. Lattice mismatch between InAs and AlAsSb is just 3.2% at 300 K (compared with 7.2% in InAs/GaAs QDs),[14] but this still provides sufficient strain to drive self-assembly.[15,16] Despite these benefits, InAs(Sb)/AlAsSb SAQDs remain unexplored.

In this letter we investigate the growth of InAs SAQDs within AlAsSb barriers on InP substrates. Our choice of binary InAs for the SAQDs simplifies growth and characterization during the initial testing of this material system. Specifically, we discuss how the structural and optical properties of InAs SAQDs are strongly dependent on the composition of $GaAs_{1-x}Sb_x$ cladding layers placed above and below the dots. Using these $GaAs_{1-x}Sb_x$ cladding layers to effectively reduce the presence of Sb adjacent to the InAs, we achieve a significant enhancement in SAQD quality.

We found during early experiments that simply depositing InAs directly onto AlAsSb resulted in samples with poor optical performance. It has been reported that in a similar material system, InAs SAQDs within AlAs barriers can be degraded by Al diffusion.[17] However, Al diffusion was inhibited by inserting a thin GaAs cladding layer between the InAs and AlAs, considerably improving photoluminescence (PL) response.[17] We therefore now incorporate analogous $GaAs_{1-x}Sb_x$ cladding layers either side of the InAs. These thin ($\leq$10 ML) layers add small perturbations to the original band structure [Fig. 1(a)]. Although changing the $GaAs_{1-x}Sb_x$ composition has negligible effect on its conduction band (CB) offset, increasing (reducing) the Sb mole-fraction, x, raises (lowers) its VB relative to InAs. Capping with $GaAs_{1-x}Sb_x$ can also change the properties of the dots themselves.[18]

To investigate the impact of adding the $GaAs_{1-x}Sb_x$ cladding layers we grew samples on InP(001) on-axis ($\pm$0.5°) substrates by solid-source molecular beam epitaxy. Substrate temperature (T_{sub}) is calibrated using reflection high-energy electron diffraction (RHEED) to observe the InP surface reconstruction transition from a Group V-stabilized 2×4 to a

a)Author to whom correspondence should be addressed. Electronic mail: p.j.simmonds.03@cantab.net.

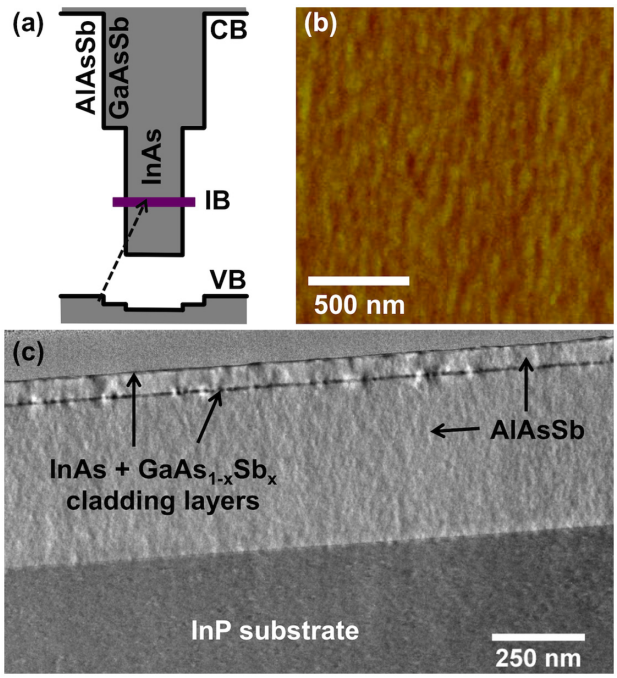

FIG. 1. (a) Schematic diagram of the InAs/$GaAs_{1-x}Sb_x$/AlAsSb band structure. The dashed arrow represents an electron transition from the VB to the IB. (b) 4 μm^2 AFM image showing typical $GaAs_{1-x}Sb_x$ surface morphology prior to InAs deposition. (c) XTEM image of the full structure showing the crystalline quality of the AlAsSb barriers and the InAs/$GaAs_{1-x}Sb_x$ layers.

Group III-stabilized 4×2 at 530 °C. We use thermally cracked As_2 and Sb_2, removing the native oxide from the InP substrates at $T_{sub} = 520$ °C under As_2 flux to prevent In-droplet formation. All samples have the following structure: at $T_{sub} = 500$ °C we grow a 400 nm AlAsSb barrier, a 5–10 ML $GaAs_{1-x}Sb_x$ cladding layer, an 8.0 ML InAs QD layer, a 5–10 ML $GaAs_{1-x}Sb_x$ cladding layer, a 50 nm AlAsSb barrier, a 5–10 ML $GaAs_{1-x}Sb_x$ cladding layer, and finally 8.0 ML InAs QDs on the surface. The samples are immediately cooled under As_2. The AlAsSb and GaAsSb layers are grown at 0.3 ML/s with V/III beam equivalent pressure (BEP) ratios of ~17 and ~11, respectively. We deposit the InAs at 0.085 ML/s with a V/III BEP ratio of ~60.

Due to wide miscibility gaps, AlAsSb and GaAsSb are highly challenging to grow.[19–21] The As/Sb incorporation ratio is extremely sensitive to small variations in growth rate and T_{sub}. In practice, we keep the Group III and Sb_2 BEPs constant and adjust the As_2 BEP to achieve the required composition. Composition is measured using x-ray diffraction (XRD). Symmetric 004 and asymmetric 224 XRD reciprocal space maps for 400 nm AlAsSb calibration samples show that these bulk layers remain fully strained to the InP substrate, even when the Sb mole fraction has drifted by as much as $\Delta x = 0.06$ from the lattice matched composition. For this study, our samples contain $GaAs_{1-x}Sb_x$ cladding layers with nominal compositions $x = 0.49$, 0.30, 0.15, and 0.

When we deposit InAs on the $GaAs_{1-x}Sb_x$ cladding layers, the RHEED pattern quickly transforms from the streaky 3×2 of GaAsSb to the streaky 2×4 of flat InAs. After deposition of ~4.75 ML InAs, the RHEED becomes spotty indicating a transition to 3D growth. These observations are consistent with Stranski-Krastanov (SK) growth where 3D self-assembly is preceded by planar wetting layer formation.

We use atomic force microscopy (AFM) to explore surface morphology and cross-sectional transmission electron microscopy (XTEM) to study the internal structure of our samples. XTEM specimens are prepared using a focused-ion beam and imaged on a FEI Titan at 300 kV. To analyze the optical properties of the buried InAs SAQDs we perform PL at 77 K with a 2.33 eV (532 nm) pump laser and at 20 K with a 1.95 eV (633 nm) pump laser. The PL signal is dispersed by a spectrometer and then collected by an extended InGaAs detector with a low-energy cut-off at 0.48 eV (2560 nm).

Prior to InAs deposition, the $GaAs_{1-x}Sb_x$ cladding layers are smooth, with typical rms roughness <3.5 Å across 25 μm^2 [Fig. 1(b)]. XTEM of the complete heterostructure [Fig. 1(c)] reveals excellent material quality. Although strain in the InAs/$GaAs_{1-x}Sb_x$ layers is locally rather large, we observe no dislocations or other defects originating in these regions. Weak contrast variation in the AlAsSb might indicate phase separation,[22] whereas the bright light and dark regions within the InAs/$GaAs_{1-x}Sb_x$ layers suggest strain modulation due to QD self-assembly.

Figure 2 shows that self-assembly of InAs QDs has indeed occurred, with morphologies that are highly dependent on the composition of the underlying $GaAs_{1-x}Sb_x$. InAs deposited onto $GaAs_{0.51}Sb_{0.49}$ (i.e., lattice matched to InP) forms dashes parallel to [01-1] and up to 500 nm long [Fig. 2(a)]. Analogous morphologies are well known during growth of InAs on InP and similar materials.[23,24] Reducing x suppresses nanostructure elongation, [Figs. 2(b)–2(d)] until for $x = 0$ (i.e., GaAs cladding layers) InAs forms quasi-circular SAQDs. The InAs SAQDs in Fig. 2(d) have areal density of 2×10^{10} cm^{-2}, are ~5 nm tall, and ~35 nm in diameter.

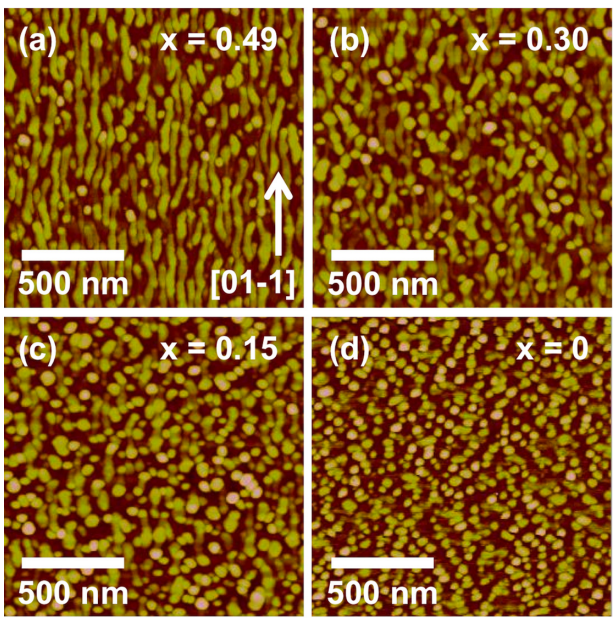

FIG. 2. 4 μm^2 AFM images showing the evolution in surface morphology of 8.0 ML InAs deposited onto $GaAs_{1-x}Sb_x$ as a function of the Sb mole fraction for: (a) $x = 0.49$, (b) $x = 0.30$, (c) $x = 0.15$, and (d) $x = 0$. The out of plane scale in each is 10 nm.

We believe the change in nanostructure shape in Fig. 2 is unrelated to the decrease in $GaAs_{1-x}Sb_x$ lattice constant as x is reduced; XTEM shows no evidence of plastic strain relaxation in the cladding layers (even when $x = 0$) and for a given value of x, InAs morphology is unaffected by raising the $GaAs_{1-x}Sb_x$ thickness from 5 to 10 ML. We instead attribute the change in InAs morphology to the fact that Sb is a known surfactant that can inhibit lateral strain relaxation processes[25] such as SK growth. As x is lowered, the effect of Sb on the interfacial surface energy is reduced and the InAs dashes shorten until, for $x = 0$, the InAs self-assembles into discrete dots. For this limiting case ($x = 0$) a negligible concentration of Sb atoms at the cladding layer surface might reasonably be expected since the GaAs spatially separates this interface from the AlAsSb. There is evidence however that Sb atoms strongly surface segregate during growth.[26] In our samples, this could lead to Sb from the AlAsSb forming a floating layer that rides the growth front of the GaAs cladding layer. Although the amount of Sb that ends up at the top GaAs surface may be too low for incorporation during subsequent InAs growth, its mere presence will still influence nanostructure formation and properties. However, despite the likelihood of surface segregation, the concentration of Sb atoms at the $GaAs_{1-x}Sb_x$/InAs interface is necessarily lowest when $x = 0$, as reflected in the improved SAQD morphology in Fig. 2(d).

Dislocated SAQDs would be deleterious to IBSC performance since mid-gap states commonly associated with dislocation cores can act as carrier recombination pathways. We search for dislocations in the InAs using XTEM and in particular the GaAs ($x = 0$) cladding layer sample since, with the largest lattice mismatch, these SAQDs are most likely to be relaxed [Fig. 3(a)]. The surface InAs SAQDs are lens-shaped in cross-section and at higher resolution [Fig. 3(b)] we see that they are coherently strained to the underlying GaAs with no evidence of dislocation formation. The three buried SAQDs in Fig. 3(a) are shown at higher resolution in Fig. 3(c) and these, like the surface dots, are also dislocation-free. SAQDs can change shape during capping,[27] explaining the apparent difference in size between surface and buried dots.

$GaAs_{1-x}Sb_x$ cladding layer composition also influences the optical activity of the InAs SAQDs [Fig. 4(a)]. For samples where $x > 0$, increasing x red-shifts the PL energy and decreases the emission intensity measured at 77 K. A 15× increase in PL intensity is obtained for the $x = 0$ sample, which is centered at ~0.87 eV with a FWHM of ~90 meV [Fig. 4(a)]. A control sample (identical to the $x = 0$ sample but containing no InAs, not shown here) has no corresponding PL emission and confirms that the bright signal at 0.87 eV from the $x = 0$ sample originates in the InAs.

Observations of red-shifted emission energy and decreased PL intensity with increasing x are consistent with studies of Sb-containing cladding layers in other material systems.[18] Ulloa *et al.* found that although $GaAs_{1-x}Sb_x$ capping layers with very low Sb content increase PL intensity from InAs/GaAs SAQDs, alloy fluctuations at higher x lead to a substantial decrease in emission intensity and red-shifting of the PL energy.[18] If x is very large, Sb diffusion into the InAs SAQDs is also an issue.[28] Our $x = 0$ sample hence emits bright PL since alloy fluctuations do not apply to binary GaAs cladding layers, and the only contribution of Sb atoms comes from surface segregation.[26] The broad PL linewidth from this sample is likely due to dispersion in SAQD size [Fig. 2(d)]. The lack of a PL signal from the InAs wetting layer in Fig. 4(a) suggests that electrons are efficiently captured by the SAQDs before they can recombine within the wetting layer itself.

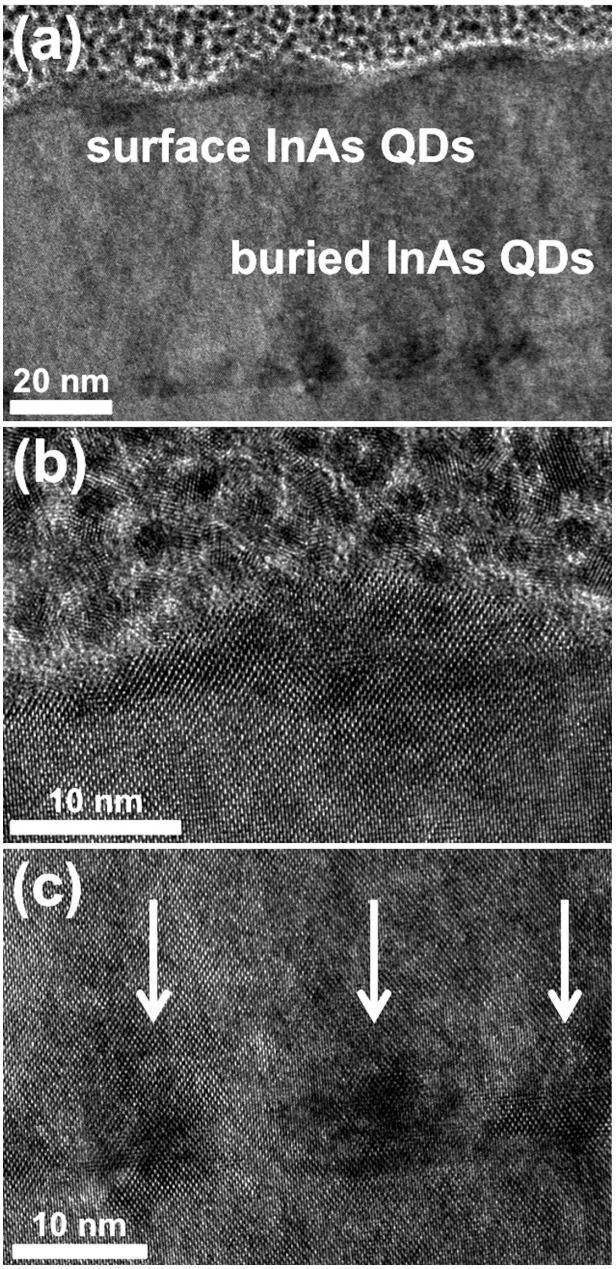

FIG. 3. Bright-field XTEM images along a {220} zone axis showing (a) surface and buried InAs with GaAs (i.e., $x = 0$) cladding layers and separated by a 50 nm AlAsSb capping layer, (b) high-resolution image of an individual surface InAs SAQD, (c) three buried InAs SAQDs at high resolution (as indicated by the arrows).

The inclusion of cladding layers alters the band structure from the original InAs(Sb)/AlAsSb SAQD design[10] [Fig. 1(a)], with the $GaAs_{1-x}Sb_x$ VB lowered as $x \to 0$. Despite this, we have confirmed that type-II behavior is maintained, even for the sample with GaAs cladding layers. At 20 K the PL peak energy from the GaAs sample shows a pronounced blue-shift that is linearly dependent on the cube

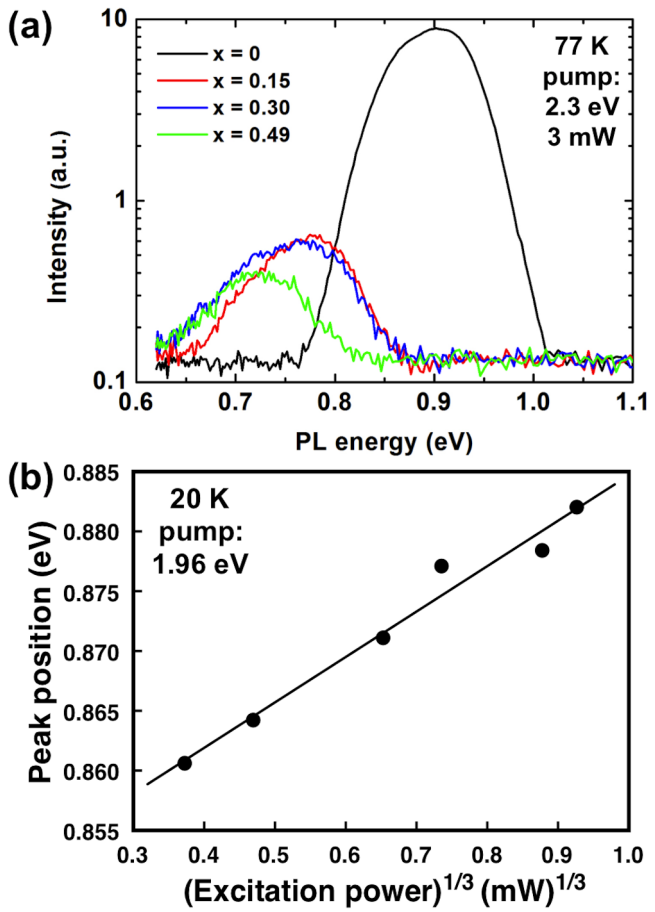

FIG. 4. (a) Dependence of PL emission at 77 K on $GaAs_{1-x}Sb_x$ cladding layer composition. (b) PL peak position at 20 K as a function of the cube root of excitation power for the sample with GaAs cladding layers.

root of the pump laser power [Fig. 4(b)]. A cube root dependence is an established characteristic of type-II heterostructures,[29,30] which means that VB perturbations due to the GaAs layers are insufficient to produce hole confinement. Instead, we find that the electrons recombine with holes in the AlAsSb barriers. Raising the thickness of the $GaAs_{1-x}Sb_x$ cladding layers from 5 to 10 ML reduces the PL intensity; PL from a sample with 10 ML $GaAs_{0.51}Sb_{0.49}$ cladding layers is ~3 times less intense than from a sample with 5 ML $GaAs_{0.51}Sb_{0.49}$ cladding layers (not shown). Increasing the $GaAs_{1-x}Sb_x$ thickness decreases the overlap between the wavefunctions of electrons in the InAs and holes in the AlAsSb and hence reduces the recombination probability.[31] If the electrons were simply recombining with holes in the $GaAs_{1-x}Sb_x$, changing the thickness of the cladding layers would have much weaker impact on PL intensity.

As well as improved SAQD morphology and brighter PL, there is an additional benefit to using GaAs cladding layers. The InAs/GaAs/AlAsSb material system possesses the inherent potential for strain compensation. Although the lattice mismatch between InAs and the GaAs cladding layers is larger than between InAs and AlAsSb, GaAs is tensilely strained to AlAsSb by 3.7%, while InAs is compressively strained to AlAsSb by 3.2%. The ability to balance compressive and tensile strain will be very useful when growing the multiple layers of SAQDs required for increased absorption cross-section in an IBSC.

Given their structural and optical properties, these InAs SAQDs show great potential for use in optoelectronic devices such as solar cells. That being said, at 0.87 eV the VB to ground state transition in our InAs SAQDs is higher than theory requires for an ideal IBSC.[3,11] There are several routes open to us by which we can reduce the emission energy. In addition, to adjusting the growth conditions (e.g., InAs growth rate, thickness, T_{sub}, and V/III BEP ratio), we will investigate $GaAs_{1-x}Sb_x$ cladding layers with compositions in the optimal range $x \leq 0.12$ found by Ulloa *et al.*[18] We also have the option of intentionally trying to create InAs(Sb) SAQDs, as per the original design of Levy *et al.*[10] Although we have seen that the presence of Sb tends to adversely affect SAQD properties, this may be offset by the fact that InAs(Sb) dots will allow us to access lower emission energies. By optimizing all these parameters we shall fine-tune the properties of the SAQDs for use in IBSCs.

We should note that our InAs SAQDs could contain one or more higher-order confined electron states far enough below the AlAsSb CB as to form additional IBs.[9] Raising the number of IBs increases the number of photon absorption paths and tends to improve IBSC efficiency.[32] However, detailed band structure calculations and low-temperature PL analysis will be required to investigate whether these additional bands exist within our samples.

In conclusion, we have investigated the role of $GaAs_{1-x}Sb_x$ cladding layers in mediating the growth of type-II InAs SAQDs inside AlAsSb barriers. As the Sb-content of the $GaAs_{1-x}Sb_x$ cladding layers is reduced to zero, the InAs morphology changes from elongated dashes into discrete, lens-shaped SAQDs. This transformation of the structural properties is accompanied by an enhancement in optical quality so that InAs SAQDs within GaAs cladding layers exhibit bright PL emission at 0.87 eV. Through further optimization, both of cladding layer composition and dot growth conditions, we expect to achieve InAs SAQDs that form an intermediate band close to 0.7 eV above the VB, the ideal position for a functional, high-efficiency IBSC.

This material is based upon work supported by the U.S. Department of Energy under Award Number DE-EE0005325.

[1]A. Luque and A. Martí, Phys. Rev. Lett. **78**, 5014 (1997).
[2]A. Luque, A. Martí, and L. Cuadra, IEEE Trans. Electron Devices **48**, 2118 (2001).
[3]A. Martí, L. Cuadra, and A. Luque, IEEE Trans. Electron Devices **48**, 2394 (2001).
[4]S. Tomić, T.S. Jones, and N.M. Harrison, Appl. Phys. Lett. **93**, 263105 (2008).
[5]A. Martí, E. Antolín, C.R. Stanley, C.D. Farmer, N. López, P. Díaz, E. Cánovas, P.G. Linares, and A. Luque, Phys. Rev. Lett. **97**, 247701 (2006).
[6]R.B. Laghumavarapu, A. Moscho, A. Khoshakhlagh, M. El-Emawy, L.F. Lester, and D.L. Huffaker, Appl. Phys. Lett. **90**, 173125 (2007).
[7]P.G. Linares, A. Martí, E. Antolín, and A. Luque, J. Appl. Phys. **109**, 014313 (2011).
[8]V. Popescu, G. Bester, M.C. Hanna, A.G. Norman, and A. Zunger, Phys. Rev. B **78**, 205321 (2008).
[9]Q. Shao, A.A. Balandin, A.I. Fedoseyev, and M. Turowski, Appl. Phys. Lett. **91**, 163503 (2007).
[10]M. Y. Levy, C. Honsberg, A. Martí, and A. Luque, in 31st IEEE Photovoltaics Specialists Conference, 3–7 January 2005, pp. 90–93.
[11]A. Luque and A. Martí, Prog. Photovoltaics **9**, 73 (2001).
[12]S.P. Bremner, M.Y. Levy, and C.B. Honsberg, Appl. Phys. Lett. **92**, 171110 (2008).

[13]M. Hayne, J. Maes, S. Bersier, V.V. Moshchalkov, A. Schliwa, L. Müller-Kirsch, C. Kapteyn, R. Heitz, and D. Bimberg, Appl. Phys. Lett. **82**, 4355 (2003).
[14]I. Vurgaftman, J.R. Meyer, and L.R. Ram-Mohan, J. Appl. Phys. **89**, 5815 (2001).
[15]D. Leonard, M. Krishnamurthy, C.M. Reaves, S.P. Denbaars, and P.M. Petroff, Appl. Phys. Lett. **63**, 3203 (1993).
[16]P.J. Simmonds and M.L. Lee, Appl. Phys. Lett. **99**, 123111 (2011).
[17]S.-K. Park, J. Tatebayashi, and Y. Arakawa, Appl. Phys. Lett. **84**, 1877 (2004).
[18]J.M. Ulloa, R. Gargallo-Caballero, M. Bozkurt, M. del Moral, A. Guzmán, P.M. Koenraad, and A. Hierro, Phys. Rev. B **81**, 165305 (2010).
[19]Y.-H. Zhang, J. Cryst. Growth **150**, 838 (1995).
[20]E. Hall, H. Kroemer, and L.A. Coldren, J. Cryst. Growth **203**, 447 (1999).
[21]G. Almuneau, E. Hall, S. Mathis, and L.A. Coldren, J. Cryst. Growth **208**, 113 (2000).
[22]B.-R. Wu, K.Y. Cheng, C. Xu, and K.-C. Hsieh, J. Vacuum Sci. Technol. B **24**, 1660 (2006).
[23]O. Bierwagen and W.T. Masselink, Appl. Phys. Lett. **86**, 113110 (2005).
[24]P.J. Simmonds, H.E. Beere, H.W. Li, P. See, A.J. Shields, and D.A. Ritchie, J. Vacuum Sci. Technol. B **25**, 1044 (2007).
[25]J.C. Harmand, L.H. Li, G. Patriarche, and L. Travers, Appl. Phys. Lett. **84**, 3981 (2004).
[26]R. Kaspi and K.R. Evans, J. Cryst. Growth **175/176**, 838 (1997).
[27]G. Costantini, A. Rastelli, C. Manzano, P. Acosta-Diaz, R. Songmuang, G. Katsaros, O. G. Schmidt, and K. Kern, Phys. Rev. Lett. **96**, 226106 (2006).
[28]S. I. Molina, A. M. Sánchez, A. M. Beltrán, D.L. Sales, T. Ben, M.F. Chisholm, M. Varela, S.J. Pennycook, P.L. Galindo, A.J. Papworth, P.J. Goodhew, and J.M. Ripalda, Appl. Phys. Lett. **91**, 263105 (2007).
[29]Y.S. Chiu, M.H. Ya, W.S. Su, and Y.F. Chen, J. Appl. Phys. **92**, 5810 (2002).
[30]Y.I. Mazur, V.G. Dorogan, G.J. Salamo, G.G. Tarasov, B.L. Liang, C.J. Reyner, K. Nunna, and D.L. Huffaker, Appl. Phys. Lett. **100**, 033102 (2012).
[31]K. Gradkowski, T.J. Ochalski, N. Pavarelli, H.Y. Liu, J. Tatebayashi, D.P. Williams, D.J. Mowbray, G. Huyet, and D.L. Huffaker, Phys. Rev. B **85**, 035432 (2012).
[32]A.S. Brown and M.A. Green, J. Appl. Phys. **94**, 6150 (2003).